PHYSICAL REVIEW B VOLUME 54, NUMBER 7 15 AUGUST 1996-I

# Strong alignment of self-assembling InP quantum dots

K. Häusler, K. Eberl, F. Noll, and A. Trampert
*Max-Planck-Institut für Festkörperforschung, 70569 Stuttgart, Germany*
(Received 6 March 1996)

We report on a mechanism for ordering of self-assembling InP quantum dots which are prepared by molecular-beam epitaxy on a strained $In_{0.61}Ga_{0.39}P$ buffer layer on (001) GaAs. A pronounced alignment of InP nanoscale clusters is observed along the ⟨110⟩ directions. This phenomenon is attributed to the diffusion of surface adatoms driven by the stress of misfit dislocations confined at the $In_{0.61}Ga_{0.39}P$/GaAs interface. [S0163-1829(96)08931-X]

## I. INTRODUCTION

Significant research effort is devoted to studying the evolution of surface morphology and the self-assembling of coherently strained islands in heteroepitaxy. Recent work has focussed on self-assembling InAs, $In_xGa_{1-x}As$ or InP islands on a GaAs substrate, because self-assembling provides a maskless technique for fabricating quantum dots with dimensions on the order of 10 nm.[1–5] The formation of islands is based on the transition from two-dimensional van der Merwe growth to three-dimensional Stranski-Krastanov (SK) growth. Due to the SK growth mode the islands nucleate on top of a wetting layer which is typically between 1 and 2 ML thick.[4] Self-assembling has been described by means of surface diffusion of atoms due to the reduction of the surface chemical potential during growth[6,7] or influenced by diffusion barriers at the island edges.[8] The driving mechanism to self-assembling is the partial elastic relaxation within the islands taking into account the surface free energy on island facets.[9,10] A challenge in the field of self-organized crystal growth is to learn how to order the self-assembling islands. Different approaches to ordering of quantum dots based on non-(001) or patterned substrates have been suggested.[11–14] Other researchers have observed an ordering of islands along short line segments either on (001) or on off-oriented GaAs.[2,12] This effect is attributed to an undulation of the surface by macrosteps which are formed during epitaxy due to step bunching.[15]

Another effect causing surface undulations originates from the strain field of misfit dislocations.[16] The mechanism to strain relaxation requires an epilayer thickness above the equilibrium critical thickness, which is characterized by the start of dislocation glide while leaving a residual strain.[17] Most of the dislocations in strain-relaxed epitaxial III-V heterostructures with small misfit (≤2%) are of 60° type, having an angle of 60° between Burgers vector and line direction. Long segments of 60° dislocations form at the interface between substrate and epilayer by dislocation nucleation or glide of threading dislocations.[18] The misfit dislocations in (001)-oriented III-V heterostructures extend along the two perpendicular ⟨110⟩ directions parallel to the surface, forming an orthogonal array at the interface between substrate and epilayer. In this paper we report on the strong alignment of InP islands caused by preferential island formation on a strained $In_{0.61}Ga_{0.39}P$ buffer layer modulated by an array of 60°-misfit dislocations.

## II. EXPERIMENT

The epitaxial layers are grown by solid-source molecular-beam epitaxy on (001) GaAs. A special GaP decomposition cell is used as phosphorus source.[19] We deposit the layers at a growth rate of 1 ML/s by applying a group-V beam equivalent pressure of typical $5\times10^{-6}$ Torr. The $In_xGa_{1-x}P$ layers are grown at a substrate temperature of 480 °C for which the surface reconstruction is (2×1). As a buffer layer we deposit a 200-nm GaAs film on the GaAs substrate followed by a 150-nm-thick strained $In_{0.61}Ga_{0.39}P$ layer. The thickness of the $In_{0.61}Ga_{0.39}P$ layer is selected at slightly above the critical thickness for plastic strain relaxation. The degree of relaxation is small, thus only a few well-separated misfit dislocations are formed at the GaAs/$In_{0.61}Ga_{0.39}P$ interface. On top of the $In_{0.61}Ga_{0.39}P$ layer we deposit 1.5 ML InP at a growth rate of 0.5 ML/s. The growth mode transition from two-dimensional growth to island formation is clearly indicated by reflection high-energy electron diffraction (RHEED) showing a spotty pattern after the deposition of 1.5 ML InP.

We have investigated the structural properties of the strained $In_{0.61}Ga_{0.39}P$ layer by double crystal x-ray diffractometry. The layer composition and the degree of relaxation are estimated from 004 and 224 x-ray rocking curves. The evaluation of x-ray data indicates that the $In_{0.61}Ga_{0.39}P$ layer is anisotropically relaxed with the degree of relaxation being about 12% into $[1\bar{1}0]$ and about 14% into [110]. Knowing the degree of relaxation we can calculate the dislocation density into the corresponding crystal direction assuming that the dislocations are of 60° type. The linear density of dislocations is $\rho_{hkl}=2\sqrt{2}R_{hkl}\epsilon_0/a_e$, where $R_{hkl}$ is the degree of relaxation into [hkl], $\epsilon_0=0.93\%$ is the lattice misfit between $In_{0.61}Ga_{0.39}P$ and GaAs, and $a_e$ is the lattice constant of the $In_{0.61}Ga_{0.39}P$ epilayer. We obtain the line density of dislocations, which is $\rho_{110}=\frac{1}{150}$ nm$^{-1}$ into [110] and $\rho_{1\bar{1}0}=\frac{1}{180}$ nm$^{-1}$ into the perpendicular direction. The second sample has a 150-nm-thick $In_{0.64}Ga_{0.36}P$ layer with higher dislocation densities of $\rho_{110}=1/60$ nm$^{-1}$ and $\rho_{1\bar{1}0}=1/100$ nm$^{-1}$.

## III. RESULTS

Figure 1 shows an atomic force microscopy (AFM) image of the InP islands on the $In_{0.61}Ga_{0.39}P$ buffer layer. The size

 © 1996 The American Physical Society

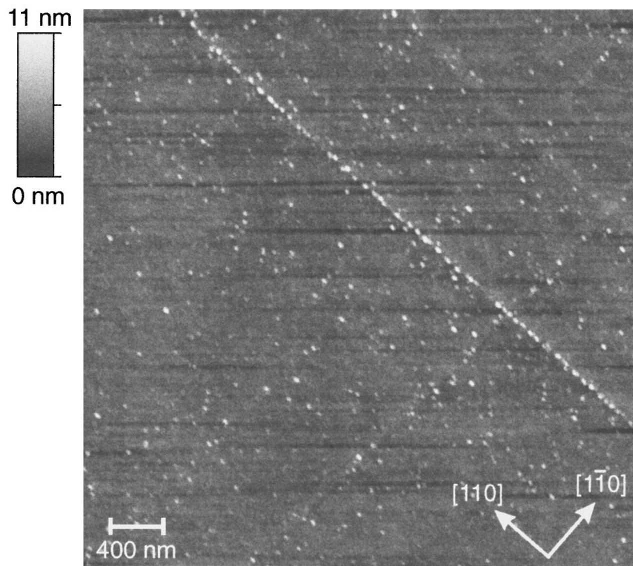


FIG. 1. Atomic force microscopy (AFM) image of an $In_{0.61}Ga_{0.39}P$ buffer layer with InP islands formed from 1.5 ML InP. Islands are accumulated on surface ridges along both $\langle 110\rangle$ directions. There is a strong alignment of lnP dots on one ridge extending along [110].

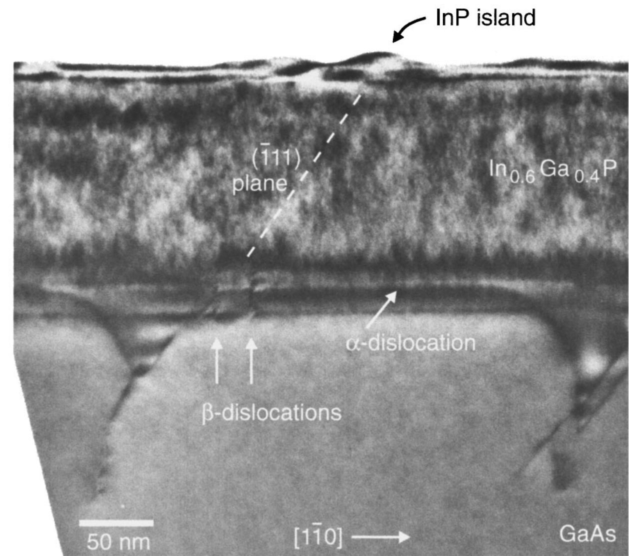


FIG. 3. Cross-sectional bright field TEM of the specimen with $\mathbf{g}=220$ excitation. The GaAs substrate, the $In_xGa_{1-x}P$ layer, and some InP islands are shown. Intersecting dislocations are seen at the $In_xGa_{1-x}P$/GaAs interface. Some dislocations extend into the substrate.

of individual InP islands varies between 20 and 30 nm in diameter and 5 and 10 nm in height. A pronounced alignment over a distance of more than 4 $\mu$m oriented along the [110] direction is observed. Also, a much weaker accumulation of islands can be seen along lines, which extend along the two orthogonal $\langle 110\rangle$ directions. We have performed AFM scans at larger and different areas of the specimen. The AFM investigations clearly indicate that the lines of accumulated islands along the $\langle 110\rangle$ directions are randomly distributed. Most of these lines are more than 50 $\mu$m long and separated by at least 1–5 $\mu$m. Nearly all islands are slightly elongated along the [110] direction, which is the direction of the highest degree of relaxation. Figure 2 indicates an AFM scan of the sample with the $In_{0.64}Ga_{0.36}P$ buffer layer having a higher dislocation density. The surface of the buffer layer shows a characteristic undulated morphology. The InP dots are preferentially nucleated on top of the surface undulations, whereas nearly no island is nuclated in the valley regions. Additionally, we observe elliptic islands, which are elongated along the direction perpendicular to the surface waves. In contrast to these dot arrangements we observe a statistical distribution of the self-assembling InP islands for lattice matched $In_{0.5}Ga_{0.5}P$ buffer layers on (001) GaAs substrate.

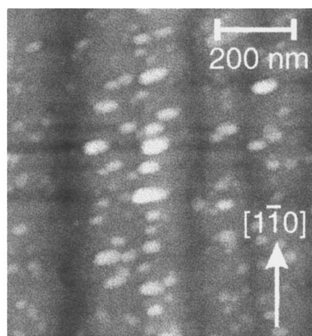


FIG. 2. AFM image of an $In_{0.64}Ga_{0.36}P$ buffer layer with InP islands. We observe a pronounced accumulation of islands on top of surface undulations. Nearly no InP dot is detected in the valleys of the undulations. The islands are elongated along [110].

Figure 3 shows a [110] cross-sectional transmission electron micrograph (TEM) of the 150-nm-thick $In_{0.61}Ga_{0.39}P$ layer on GaAs substrate. The specimen has been tilted by nearly 30° around the [1$\bar{1}$0] axis to image the dislocation network. At the $In_{0.61}Ga_{0.39}P$/GaAs interface we observe misfit dislocations. We distinguish between misfit dislocations parallel to [1$\bar{1}$0], so called $\alpha$ dislocations and dislocations into the [110] direction which are $\beta$ dislocations. The in-plane dislocations shown in Fig. 3 are $\alpha$ dislocations, whereas the short segments marked by arrows correspond to $\beta$ dislocations. In addition, we observe V-shaped inclined tips and threading dislocations extending into the substrate. The distance of the two $\beta$ dislocations is about 20 nm; however, the distance to the next accumulated $\beta$ dislocations is on the order of several hundred nanometers. Similar arrangements of accumulated $\beta$ dislocations have been observed for strain-relaxed III-V compounds by Lefebvre and Ulhaq-Bouillet.[20] They proposed a dislocation multiplication mechanism which produces closely spaced $\beta$ dislocations with identical Burgers vectors by formation of the typical V-shaped tips and dislocation loops extending deep into the substrate. On top of the $In_{0.61}Ga_{0.39}P$ buffer layer we observe the InP islands. TEM micrographs from different areas of the specimen show a preferential arrangement of the islands in the vicinity of accumulated $\beta$ dislocations. A typical configuration is shown in Fig. 3. Islands are observed near the intersection between a (111) glide plane and the surface.

The correlation between misfit dislocations and the alignment of islands is confirmed by the evaluation of the AFM height profile shown in Fig. 1. We determine the areal density $\rho(\mathbf{r})=h(\mathbf{r})/\Omega$ of InP lattice sites in the volume of islands, where $h(\mathbf{r})$ is the height profile of islands at the place

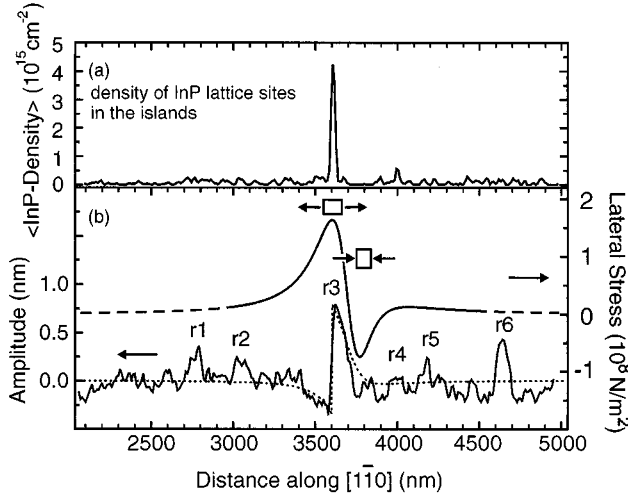


FIG. 4. (a) The areal density of InP lattice sites in the islands obtained from Fig. 1 averaged along [110] is plotted against the distance from the left lower corner of the AFM image along [1$\bar{1}$0]. The peak at 3600 nm indicates the position of the strongly aligned islands. (b) The averaged AFM amplitude of the buffer layer without the islands (lower curve, solid line) fits to the surface displacement (dotted line) of four dislocations placed at about 3700 nm. The upper curve indicates the lateral stress of InP cells on the surface originating from the four dislocations. Compressively strained and tensile regions are indicated.

**r** on the surface and $\Omega$ is the volume of a lattice site. Figure 4(a) shows the areal density of InP lattice sites averaged along [110] plotted against the [1$\bar{1}$0] direction. The maximum density corresponding to the aligned islands is $4.2\times10^{15}$ cm$^{-2}$, whereas the density averaged over the whole area is $1.2\times10^{14}$ cm$^{-2}$ due to 0.2 ML InP. The surface profile of the $In_{0.61}Ga_{0.39}P$ buffer layer as shown in Fig. 4(b) is determined from the AFM image after subtracting the InP islands. The surface amplitude averaged along [110] is plotted against the [1$\bar{1}$0] direction perpendicular to the lines of islands. There are at least six ridges $r1 \ldots r6$ with an amplitude above the noise level. Between the ridges $r1$ and $r2$ there is a weak accumulation of small islands with an InP density of $2\times10^{14}$ cm$^{-2}$. The surface ridge $r3$ with the largest amplitude corresponds to the position of the aligned islands. In addition, there is a weak accumulation of islands with a maximum InP density of $5.6\times10^{14}$ cm$^{-2}$ between $r4$ and $r5$. The ridge $r6$ has only half of the amplitude of $r3$ but it is not correlated to any significant island accumulation. The dotted line fitting the shape of the ridge $r3$ indicates the surface displacement of four closely spaced $\beta$ dislocations at the $In_{0.61}Ga_{0.39}P$/GaAs interface calculated in isotropic elasticity. The ridges $r1$, $r2$, $r4$, and $r5$ originate from single dislocations, and $r6$ has the same amplitude as two accumulated $\beta$ dislocations. The symmetric shape of $r6$ indicates, that this ridge probably originates from two dislocations having different orientation of the Burgers vector.

There is also a weak accumulation of islands along the perpendicular [1$\bar{1}$0] direction. Figures 5(a) and 5(b) indicate the density of InP and the amplitude of the buffer layer plotted against [110] both averaged along [1$\bar{1}$0]. The amplitude shows three ridges corresponding to single $\alpha$ dislocations and one ridge due to two accumulated $\alpha$ dislocations. We observe an accumulation of islands with an averaged density of about $3\times10^{14}$ InP sites per cm$^2$ in the vicinity of the two closely spaced $\alpha$ dislocations, but there is not any accumulation near the single dislocations.

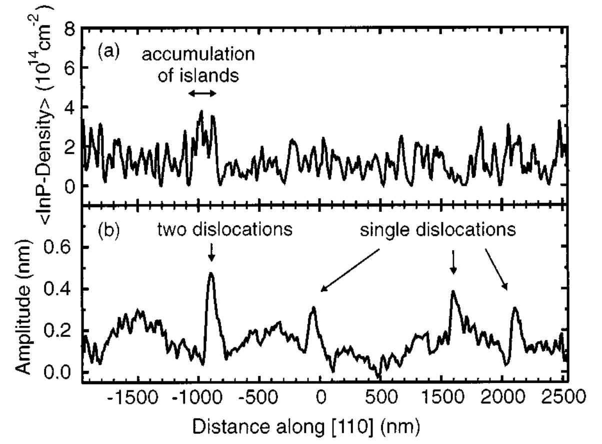


FIG. 5. (a) The areal density of InP lattice sites and (b) the surface profile obtained from the image in Fig. 1 both averaged along [1$\bar{1}$0] are plotted against the distance from the left lower corner of the AFM image along [110]. There is a weak accumulation of islands near two closely spaced dislocations but no accumulation at the surface steps of single dislocations.

## IV. DISCUSSION

We will discuss the correlation between atomic displacement on the surface and the stress field of misfit dislocations. The 60°-misfit dislocations cause an undulation of the surface originating from displacements and strain fields. The surface displacement of a single straight 60° dislocation is produced by glide of threading segments or dislocation loops. For example, if a dislocation loop with a Burgers vector $\mathbf{b}=a/2[\bar{1}01]$ glides on a $(\bar{1}11)$ plane from the surface towards the substrate, a surface step along [110] with the height $a/2$ is formed, where $a$ is the lattice constant. The corresponding profile of the step depends on the distance $d$ between the misfit dislocation and the surface. We have calculated the surface profile in the isotropic approximation applying a complex Airy stress function $\Phi$ as described by Muskhelishvili.[14] The stress function $\Phi$ is determined using the method of image dislocations.[15] We obtain the stress function,

$$\Phi(z)=\frac{b\mu}{4\pi(1-\nu)}\left[[-i(z+i)e^{i\varphi}+i(\bar{z}-i)e^{-i\varphi}]\ln\left(\frac{z+i}{z-i}\right)\right.$$
$$\left.-2\frac{\bar{z}-i}{z-i}\,e^{i\varphi}\right], \qquad (1)$$

where $b$ is the length of the Burgers vector, $\mu$ is the shear modulus, $\nu$ is the Poisson ratio, $\varphi$ is the angle between surface and glide plane, and $z=x+iy$. The coordinates $x$ and $y$ are the distances in [110] and [001] in units of the distance $d$ between the surface and a dislocation located at $z=-i$ and extending into [1$\bar{1}$0]. It can be easily shown that the real part of $\Phi$ is a biharmonic function because it has the form $\Phi=\Psi\bar{z}+\chi$, where $\psi$ and $\chi$ are analytic. Then, the function

$\Phi$ allows us to determine both the stress tensor $\sigma_{ij}$ and the complex displacement $u+iv$ using the following equations:

$$\sigma_{xx}+\sigma_{yy}=4\mathrm{Re}\left[\frac{d}{dz}\Psi(z)\right],$$

$$\sigma_{yy}-\sigma_{xx}+2i\sigma_{xy}=2\frac{d^2}{dz^2}\Phi(z), \tag{2}$$

and

$$2\mu(u+iv)=(3-4\nu)\Psi-\frac{d}{d\bar{z}}\bar{\Phi}(\bar{z}).$$

A straightforward calculation results in the surface displacement (at $y=0$):

$$u+iv=\frac{b}{\pi}\left[e^{-i\varphi}\arctan(x)-e^{i\varphi}\frac{x+i}{x^2+1}\right], \tag{3}$$

which does not depend on the elastic constants, and the surface stress,

$$\sigma_{xx}=\frac{4b\mu}{\pi(1-\nu)}\frac{x}{(1+x^2)^2}[x\cos(\varphi)-\sin(\varphi)], \tag{4}$$

which is propoprtional to $1/d$. Other components of the stress tensor at the surface are $\sigma_{xy}=\sigma_{yy}=\sigma_{zy}=0$ and $\sigma_{zz}=\nu\sigma_{xx}$, not taking into account the screw component of the dislocation. For a 60° dislocation we get $b\cos(\varphi)=a/(2\sqrt{2})$ and $b\sin(\sigma)=a/2$.

We have plotted the total displacement $v$ (dotted line) and the lateral stress $\sigma_{xx}$ (upper curve) of InP cells on the buffer layer distorted by four dislocations with Burgers vector $a/2$ $[\bar{1}01]$ and with $[110]$ line direction in Fig. 4(b). The stress $\sigma_{xx}$ is obtained by inserting the elastic constants $\mu=2.23\times10^{10}$ J/m$^3$ and $\nu=0.360$ for InP into Eq. (4). We additionally introduce the discontinuity in the calculated displacement $v$ to include the step originating from dislocation glide on the $(\bar{1}11)$ plane. The AFM profile for the large surface ridge $r3$ fits well to the calculated displacement of four closely spaced $\beta$ dislocations.

Due to the Stransky-Krastanov growth mode the formation of coherently strained islands is correlated to the smaller energy of the islands than the energy of the flat film. We will estimate the difference in the strain energy $\Delta W$ of an InP unit cell on the strained $In_{0.61}Ga_{0.39}P$ and an InP cell on the ridge of a dislocation. The energy difference is

$$\Delta W=\tfrac{1}{2}\epsilon_{ij}\sigma_{ij}-W_0\approx\epsilon_0(1+\nu)\sigma_{xx}, \tag{5}$$

neglecting the screw component, where $W_0=2\mu(1+\nu)/(1-\nu)\epsilon_0^2$ is the strain energy of an InP cell on GaAs and $\epsilon_0=0.0367$ is the lattice mismatch between InP and GaAs. The maximum stress $\sigma_{xx}$ of InP placed at the step of one dislocation is $4.1\times10^7$ J/m$^3$. By Eq. (5) we obtain the energy difference $\Delta W=8.2\times10^6$ J/m$^3$ in the case of four dislocations being 6.4% of the energy $W_0$.

In the following we consider the influence of the mass transport in the 1.5-ML-thick InP film along the surface *before* the islands are formed. As indicated by RHEED the wetting layer first grows two dimensionally, then the islands

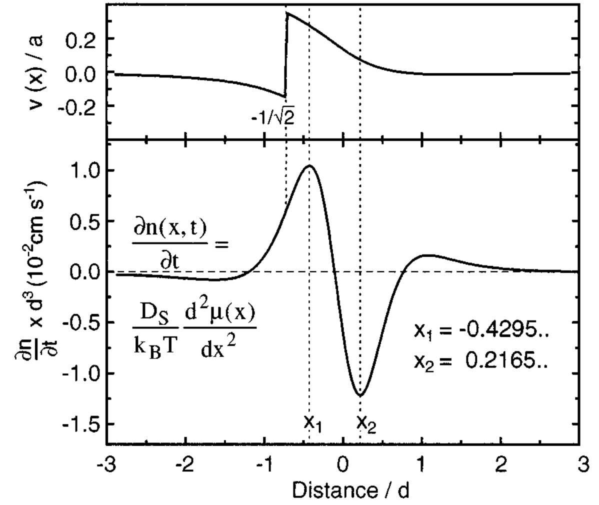


FIG. 6. The change in the local density of the wetting layer $(\partial n/\partial t)d^3$ (lower curve) calculated by Eq. (6) is plotted against the lateral distance $x/d$ from the dislocation, where $d$ is the distance between dislocation and surface. The upper curve indicates the surface displacement of the dislocation located at zero. The wetting layer is accumulated at $x_1$ and it is depleted at $x_2$ due to diffusion of surface adatoms. The parameters are $D_s=8.45\times10^{-6}\exp(-0.83$ eV/kT) cm$^2$/s and $T=480$ °C.

evolve several seconds *after* the deposition of the InP film. Therefore, we assume diffusion of atoms in the wetting layer along the $x$ direction perpendicular to the surface ridge of a 60°-misfit dislocation by neglecting three-dimensional growth in the initial stage of epitaxy. Following the Nernst-Einstein relation the surface flux of atoms is proportional to the gradient of the chemical potential on the surface. After Srolovitz[6] the chemical potential of a nonuniformly stressed solid on the surface is

$$\mu(x)=\mu_0+\gamma\kappa(x)\Omega+\tfrac{1}{2}\epsilon_{ij}(x)\sigma_{kl}(x)\Omega, \tag{6}$$

where $\mu_0$ is the chemical potential of the unstressed surface, $\gamma$ is the surface energy, $\kappa$ is the curvature of the film, and $\Omega$ is the volume of a lattice site. The surface flux leads to a time-dependent change in the local density $n(x,t)$ of the atoms given by the rate equation and the Nernst-Einstein equation

$$\frac{\partial n(x,t)}{\partial t}=-\nabla\cdot\mathbf{J}(x,t)+F\approx-\frac{D_S\delta}{k_BT}\Omega\epsilon_0(1+\nu)\frac{\partial^2\sigma_{xx}}{\partial x^2}+F, \tag{7}$$

where $\mathbf{J}$ is the flux along the surface, $F$ is the atomic flux from the vapor phase onto the surface, $D_s$ is the surface diffusivity, $\delta$ is the density of lattice sites, and $k_BT$ is the thermal energy. In Eq. (7) we neglect the influence of the curvature since $\gamma\kappa$ ($\gamma\approx2$ J/m$^2$) is smaller than $2.2\times10^4$ J/m$^3$ which is small compared to the maximum strain energy $\Delta W$ [Eq. (5)]. Figure 6 shows the surface profile of the dislocation placed at zero and the normalized rate $d^3\partial n/\partial t$ for zero flux ($F=0$) plotted against the normalized distance $x/d$ from the dislocation. By using this normalization all quantities are independent on the thickness $d$ of the buffer layer. We assume the diffusivity $D_s=8.45\times10^{-6}$ exp(−0.83 eV/kT) cm$^2$/s of the In atoms on $In_xGa_{1-x}P$ as proposed for the

growth of Ge islands on Si.[7] The wetting layer is accumulated near the maximum rate at $-0.43d$ and it is depeleted near $0.22d$. The regions of accumulation or depletion extend in a range on the order of the layer thickness $d=150$ nm. The distance between step edge and the region of highest density is about 40 nm, and between the step and the region of smallest density it is about 140 nm. For a single dislocation the maximum of $\partial n/\partial t$ is $3.1\times10^{12}$ cm$^{-2}$ s$^{-1}$ and the minimum is $-3.6\times10^{12}$ cm$^{-2}$ s$^{-1}$. After the deposition of 1.5 ML InP the averaged density of lattice sites in the wetting layer is $n_0=8.7\times10^{14}$ cm$^{-2}$. If we assume a diffusion time of $\tau=$ 10 s *ad hoc* and a lateral stress $\sigma_{xx}$ for the four accumulated dislocations we find the maximum density $n=n_0+\tau\partial n/\partial t$ of $9.9\times10^{14}$ cm$^{-2}$, which is 1.7 ML InP in the vicinity of the step edge and the minimum density of $7.3\times10^{14}$ cm$^{-2}$ being about 1.3 ML.

For InP deposition on an unstrained $In_xGa_{1-x}P$ buffer the islands start to nucleate when the wetting layer is at least 1.5 ML thick.[14] The island density strongly depends on the film thickness above the critical thickness for island formation. For example, in the case of InAs on GaAs the island density is two orders of magnitude higher for an InAs coverage of 1.75 ML than the density for 1.55 ML.[3] Therefore, we expect a pronounced accumulation of islands in the vicinity of the step edge and the depletion of islands at a distance of 140 nm apart from the step edge originating from the density fluctuations in the wetting layer. The comparison with the experimental data (see Fig. 1 and Fig. 4) indicate that there is a region between 130 and 230 nm distance from the step $r3$ where the density of islands is nearly zero.

Furthermore, there may be an influence of the step edges on the alignment of self-assembling islands similar to the alignment of InAs islands along short segments at macrosteps.[3] First, the step edge causes an energy barrier to diffusion (Schwoebel barrier).[15] Second, the binding energy of an atom is lower at a step edge than in the flat region beside the step.[9] However, our experimental data indicate that the step edge of a single or double dislocation does not cause any alignment of islands along any $\langle 110\rangle$ direction. In the vicinity of some smaller steps there is an accumulation of islands but no alignment. In this case, the island accumulation originates from the larger density of the wetting layer on the ridge. Since the position of the strongly aligned islands on the ridge $r3$ coincides with the macrostep of the four accumulated $\beta$ dislocations, it is probable that this macrostep additionally influences the position of the islands, most likely, originating from the pronounced curvature $\kappa$ of this macrostep [see Eq. (6)].

Therefore, we conclude, that the nucleation of islands is favored by the surface diffusion of the wetting layer in the stress field of accumulated misfit dislocations. Additionally, the elongated shape of islands along the direction of the highest degree of plastic strain relaxation indicates that the anisotropic surface stress influences even the three-dimensional growth of the islands. This modulation of the local growth rate may also influence the evolution of ''cross hatching,'' i.e., the surface roughness of thick strain-relaxed buffer layers.

## V. CONCLUSIONS

In summary, we have described a mechanism for ordering of nanoscale InP islands on strained $In_xGa_{1-x}P$ buffer layers on GaAs substrate. The InP clusters are accumulated on top of surface ridges aligned into the $\langle 110\rangle$ crystal directions. A calculation of the surface displacement using the Airy stress function in the isotropic approximation shows that the surface undulations which cause the strong alignment along [110] originate from multiple dislocations with the same Burgers vector. We attribute the preferential nucleation of InP clusters on top of the surface ridges to density fluctuations in the wetting layer originating from the diffusion of surface adatoms in the stress field of misfit dislocations. Within the scope of the presented data we conclude that the self-organized accumulation of islands reflects the local modulation of stress on the surface.

## ACKNOWLEDGMENTS

We gratefully acknowledge A. Kurtenbach and T. Kaneko for helpful discussions and K. Tötemeyer for technical support.

*Electronic address: haeusler@servix.mpi-stuttgart.mpg.de

[1] J. Y. Marzin, J. M. Gerard, A. Izrael, D. Barrier, and G. Bastard, Phys. Rev. Lett. **73**, 716 (1994).

[2] P. M. Petroff and S. P. Den Baars, Superlatt. Microstruct. **15,** 15 (1994).

[3] D. Leonard, K. Pond, and P. M. Petroff, Phys. Rev. B **50**, 11 687 (1994).

[4] A. Kurtenbach, K. Eberl, and T. Shitara, Appl. Phys. Lett. **66**, 361 (1995).

[5] K. Eberl, A. Kurtenbach, K. Häusler, F. Noll, and W. W. Rühle, in *Strained Layer Epitaxy,* edited by J. Bean, E. A. Fitzgerald, J. Hoyt, and K. Y. Cheng, MRS Symposia Proceedings No. 379 (Materials Research Society, Pittsburgh, 1995), p. 379.

[6] D. J. Srolovitz, Acta Metall. **37**, 621 (1989).

[7] B. J. Spencer, P. W. Voorhess, and S. H. Davis, Phys. Rev. Lett. **67**, 26 (1991).

[8] C. Ratsch, A. Zangwill, and P. Smilauer, Surf. Sci. **314**, L937 (1994).

[9] N. Grandjean, J. Massies, and F. Raymond, Jpn. J. Appl. Phys. **33**, L1427 (1994).

[10] V. A. Shchukin, N. N. Ledentsov, P. S. Kop'ev, and D. Bimberg, Phys. Rev. Lett **75**, 16 (1995).

[11] R. Nötzel, T. Fukui, H. Hasegawa, J. Temmyo, and T. Tamamura, Appl. Phys. Lett. **65**, 2854 (1994).

[12] Oshinowo, S. Tsukamoto, M. Nishinoka, and Y. Arakawa, Appl. Phys. Lett. **64**, 1221 (1994).

[13] A. Madhukar, P. Chen, Q. Xie, A. Konkar, T. R. Ramachandran, N. P. Kobayashi, and R. Viswanathan, in *Low Dimensional Structures Prepared by Epitaxal Growth or Regrowth on Patterned Substrates*, Vol. 298 of *NATO Advanced Study Institute, Series E: Natural Sciences* edited by K. Eberl, P. M. Petroff, P. Demeester (Kluwer, Dordrecht, 1995).

[14] D. S. L Mui, D. Leonard, L. A. Coldren, and P. M. Petroff, Appl. Phys. Lett. **66**, 1620 (1995).

[15] R. L. Schwoebel, J. Appl. Phys. **40**, 614 (1969).

[16] M. A. Lutz, R. M. Feenstra, F. K. LeGouess, P. M. Mooney, and

J. O. Chu, Appl. Phys. Lett. **66**, 724 (1995).
[17] J. W. Matthews and A. E. Blakeslee, J. Cryst. Growth **27**, 118 (1974).
[18] E. A. Fitzgerald, Mater. Sci. Rep. **7**, 87 (1991).
[19] T. Shitara and K. Eberl, Appl. Phys. Lett. **65**, 356 (1994).
[20] A. Lefebvre and C. Ulhaq-Bouillet, Philos. Mag. A **70**, 999 (1994).
[21] N. I. Muskhelishvili, *Some Basic Problems of the Theory of Elasticity*, translation of the third Russian edition by J. R. M. Radok (Noordhoff, Groningen, Netherlands, 1953).
[22] J. P. Hirth and J. Lothe, *Theory of Dislocations*, 2nd ed. (Wiley, New York, 1982).